ISSN 1070-3284, Russian Journal of Coordination Chemistry, 2019, Vol. 45, No. 12, pp. 867–875. © Pleiades Publishing, Ltd., 2019.
Russian Text © The Author(s), 2019, published in Koordinatsionnaya Khimiya, 2019, Vol. 45, No. 12, pp. 746–755.

Cu(II), Ni(II), and Co(II) Complexes of Tetradentate Azomethine Ligands: Chemical and Electrochemical Syntheses, Crystal Structures, and Magnetic Properties

T. V. Lifintseva[a], A. S. Burlov[b, *], V. G. Vlasenko[c], Yu. V. Koshchienko[b], D. A. Garnovskii[d], S. A. Mashchenko[b], S. I. Levchenkov[a, d], V. A. Lazarenko[e], V. N. Khrustalev[e, f], and A. L. Trigub[e]

[a]*Southern Federal University, Rostov-on-Don, Russia*
[b]*Research Institute of Physical and Organic Chemistry, Southern Federal University, Rostov-on-Don, Russia*
[c]*Research Institute of Physics, Southern Federal University, Rostov-on-Don, Russia*
[d]*Southern Scientific Center, Russian Academy of Sciences, Rostov-on-Don, Russia*
[e]*Kurchatov Institute Russian Research Center, Moscow, 123182 Russia*
[f]*Peoples Friendship University, Moscow, 117198 Russia*
**e-mail: anatoly.burlov@yandex.ru*

Received April 19, 2019; revised July 18, 2019; accepted July 22, 2019

Abstract—Complexes $CuL^1 \cdot MeOH$ (**Ia**), $NiL^1 \cdot MeOH$ (**Ib**), $CoL^1 \cdot MeOH$ (**Ic**), CuL^2 (**IIa**), NiL^2 (**IIb**), and CoL^2 (**IIc**) of the tetradentate azomethine compounds, namely, 4-methyl-*N*-[2-[(*E*)-2-[2-[2-[(*E*)-[2-(*p*-toluenesulfamino)phenyl]methyleneamino]ethoxy]ethyliminomethyl]phenyl]benzenesulfamide (H_2L^1) and 4-methyl-*N*-[2-[(*E*)-3-[4-[3-[(*E*)-[2-(*p*-toluenesulfamino)phenyl]methyleneamino]propoxy]butoxy]-propyliminomethyl]phenyl]benzenesulfamide (H_2L^2), which are the condensation products of 2-(*N*-tosylamino)benzaldehyde with 3,4-dioxa-1,8-octanediamine and 4,9-dioxa-1,12-dodecanediamine, are synthesized using the chemical and electrochemical methods. The structures, compositions, and properties of the synthesized metal complexes are studied by the methods of elemental analysis, IR spectroscopy, X-ray absorption spectroscopy, magnetochemistry, and X-ray diffraction analysis (CIF files CCDC nos. 1910746 (**Ia**), 1910747 (**Ib**), and 1910748 (**Ic**)). In the molecules of compounds **Ia**–**Ic**, the L^1 macrocyclic ligand coordinates the metal atom by four nitrogen atoms via the tetradentate chelate mode to form the polyhedron as a distorted tetrahedron.

Keywords: tetradentate Schiff bases, electrochemical synthesis, metal complexes, magnetic properties, X-ray diffraction analysis

DOI: 10.1134/S1070328419120054

INTRODUCTION

Metal complexes containing Schiff bases with various donor centers as ligands attract attention due to their diverse application as catalysts of many reactions [1–3] and functional materials with interesting photo- and electroluminescence [4–7] and magnetic characteristics [8–12]. The transition metal complexes with chelating ligands bearing O,N,S-donor atoms exhibit wide biological activity and can be used as new structural probes in the chemistry of nucleic acids and as therapeutic agents [13–15]. Numerous examples of investigations of the metal complexes of the Schiff bases as anticancer, antiviral, and antifungal drugs are known [16–20].

The Schiff base complexes of copper, nickel, cobalt, and other metals play an important role in both synthetic and structural studies due to their preparative accessibility and structural diversity caused by many modes for binding ligands to metal ions.

In this work, we synthesized the Cu(II), Ni(II), and Co(II) complexes of the tetradentate ligands, the condensation products of 2-*N*-tosylaminobenzaldehyde with 3,4-dioxa-1,8-octanediamine and 4,9-dioxa-1,12-dodecanediamine, by the chemical (from metal acetates) and electrochemical (by the anodic dissolution of the metal) methods in order to study their atomic structures and magnetic properties.

EXPERIMENTAL

Commercially available 3,6-dioxa-1,8-octanediamine, 4,9-dioxa-1,12-dodecanediamine, copper acetate monohydrate, and nickel and cobalt acetate tetrahydrates (Alfa Aesar) were used. 2-(*N*-Tosyl-

amino)benzaldehyde was synthesized using a described procedure [21].

The azomethine compounds 4-methyl-*N*-[2-[(*E*)-2-[2-[2-[(*E*)-[2-(*p*-toluenesulfamino)phenyl]methyleneamino]ethoxy]ethyliminomethyl]phenyl]benzenesulfamide (H_2L^1) and 4-methyl-*N*-[2-[(*E*)-3-[4-[3-[(*E*)-[2-(*p*- toluenesulfamino)phenyl]methyleneamino]propoxy]butoxy]propylaminomethyl]phenyl]benzenesulfamide (H_2L^2) were synthesized and described earlier [4].

Synthesis of complexes I and II by the chemical method (CM). A solution of copper acetate monohydrate (0.20 g, 0.5 mmol) or nickel acetate tetrahydrate (0.25 g, 0.5 mmol), or cobalt acetate tetrahydrate (0.25 g, 0.5 mmol) in methanol (10 mL) was added to a solution of ligand H_2L^1 (0.33 g, 0.5 mmol) or ligand H_2L^2 (0.36 g, 0.5 mmol), respectively, in methanol (20 mL). The mixture was refluxed for 2 h. Complexes **Ia**–**Ic** and **IIa**–**IIc** precipitated on cooling were washed with methanol (two times by 2 mL), recrystallized from a methanol–chloroform (2 : 1) mixture, and dried in a vacuum drying box at 150°C.

Synthesis of complexes I and II by the electrochemical method (EM) was carried out according to the standard classical procedure [22] using an EG&GPAR/173 potentiostat in a methanol–acetonitrile (1 : 1) solution with the platinum electrode as a cathode and the metal (Cu, Co, or Ni) plate as an anode. The working solution (25 mL) contained H_2L^1 (0.33 g, 0.5 mmol) or H_2L^2 (0.36 g, 0.5 mmol) and Et_4NClO_4 (0.020 g) as a current conducting additive. Electrolysis was carried out in a U-like tube with undivided cathodic and anodic spaces at a current rate of 16 mA and an initial voltage of 10 mV for 1.3 h. After the end of electrolysis, the formed precipitates of the complexes were filtered off, recrystallized from a methanol–chloroform (2 : 1) mixture, and dried in a vacuum drying box at 150°C.

Single crystals of complexes **Ia**–**Ic** were grown from a methanol–chloroform (2 : 1) mixture. X-ray diffraction analysis (XRD) was carried out for the crystals precipitated from a solution without further drying due to which the complexes with solvate (MeOH) were obtained.

Complex Ia: lilac-red crystals, yields 0.31 g (85% CM) and 0.32 g (89% EM), mp > 300°C.

For $C_{35}H_{40}N_4O_7S_2Cu$

Anal. calcd., %	C, 55.58	H, 5.33	N, 7.41	Cu, 8.40
Found, %	C, 55.42	H, 5.15	N, 7.48	Cu, 8.50 (CM)
	C, 55.45	H, 5.25	N, 7.42	Cu, 8.57 (EM)

IR (ν, cm^{-1}): 1634 ν(CH=N), 1259, 1288 $\nu_{as}(SO_2)$, 1135 $\nu_s(SO_2)$. μ_{eff} = 1.84 μ_B (294 K).

Complex Ib: light green crystals, yields 0.31 g (86% CM) and 0.32 g (90% EM), mp > 300°C.

For $C_{35}H_{40}N_4O_7S_2Ni$

Anal. calcd., %	C, 55.94	H, 5.36	N, 7.46	Ni, 7.81
Found, %	C, 56.12	H, 5.45	N, 7.50	Ni, 7.92 (CM)
	C, 56.20	H, 5.38	N, 7.52	Ni, 7.90 (EM)

IR (ν, cm^{-1}): 1625 ν(CH=N), 1260, 1302 $\nu_{as}(SO_2)$, 1133 $\nu_s(SO_2)$. μ_{eff} = 3.19 μ_B (294 K).

Complex Ic: red-brown crystals, yields 0.30 g (82% CM) and 0.32 g (90% EM), mp > 300°C.

For $C_{35}H_{40}N_4O_7S_2Co$

Anal. calcd., %	C 55.92	H 5.36	N, 7.45	Co, 7.84
Found, %	C, 56.18	H, 5.28	N, 7.32	Co, 7.95 (CM)
	C, 56.32	H, 5.20	N, 7.34	Co, 7.98 (EM)

IR (ν, cm^{-1}): 1624 ν(CH=N), 1256 $\nu_{as}(SO_2)$, 1133 $\nu_s(SO_2)$. μ_{eff} = 4.70 μ_B (294 K).

Complex IIa: lilac-red powder, yields 0.33 g (87% CM) and 0.35 g (90% EM), mp > 270°C.

For $C_{37}H_{44}N_4O_6S_2Cu$

Anal. calcd., %	C, 57.83	H, 5.77	N, 7.29	Cu, 8.27
Found, %	C, 58.91	H, 5.81	N, 7.35	Cu, 8.30 (CM)
	C, 58.79	H, 5.69	N, 7.24	Cu, 8.32 (EM)

IR (ν, cm^{-1}): 1629 ν(CH=N), 1257, 1288 $\nu_{as}(SO_2)$, 1136 $\nu_s(SO_2)$. μ_{eff} = 2.09 μ_B (294 K).

Complex IIb: green powder, yields 0.31 g (80% CM) and 0.33 g (87% EM), mp > 270°C.

For $C_{37}H_{44}N_4O_6S_2Ni$

Anal. calcd., %	C, 58.20	H, 5.81	N, 7.34	Ni, 7.69
Found, %	C, 58.23	H, 5.79	N, 7.40	Ni, 7.72 (CM)
	C, 58.29	H, 5.83	N, 7.32	Ni, 7.78 (EM)

IR (ν, cm^{-1}): 1623 ν(CH=N), 1251, 1304 $\nu_{as}(SO_2)$, 1127 $\nu_s(SO_2)$. μ_{eff} = 3.34 μ_B (294 K).

Complex IIc: red-brown powder, yields 0.31 g (80% CM) and 0.32 g (85% EM), mp > 270°C.

For $C_{37}H_{44}N_4O_6S_2Co$

Anal. calcd., %	C, 58.18	H, 5.81	N, 7.34	Co, 7.72
Found, %	C, 58.23	H, 5.87	N, 7.38	Co, 7.80 (CM)
	C, 58.20	H, 5.83	N, 7.40	Co, 7.79 (EM)

IR (ν, cm^{-1}): 1618 ν(CH=N), 1254 $\nu_{as}(SO_2)$, 1129 $\nu_s(SO_2)$. μ_{eff} = 4.72 μ_B (294 K).

X-ray absorption spectroscopy. The X-ray Cu, Ni, and Co *K*-edge absorption spectra for complexes **IIa**, **IIb**, and **IIc** were obtained in the transmission mode on an EXAFS spectrometer of the Structural Materials Science station at the Kurchatov Center of Synchrotron Radiation and Nanotechnologies (Moscow)

[23]. The energy of the electron beam used as a source of X-ray synchrotron radiation was 2.5 GeV at a current of 100–140 mA. A two-crystal Si(111) monochromator was used for the monochromatization of X-ray radiation. The EXAFS (extended X-ray absorption fine structure) spectra were processed using standard procedures of background isolation, normalization to the jump of the K edge, and atomic absorption (μ_0) isolation [24], after which the Fourier transformation of the isolated EXAFS (χ) spectra was performed in the range of wave vectors of photoelectrons (k) from 2.5 to 13.0 Å^{-1} with the weight function k^3. The obtained module Fourier transformant (MFT) was the pseudo-radial distribution of the atoms of the nearest coordination spheres around the absorbing metal atom. The threshold ionization energy (E_0) was chosen from the maximum of the first derivative of the K edge. The exact values for parameters of the structure of the nearest environment of the metal ions in the complexes were determined by the nonlinear fitting of the parameters of the corresponding coordination spheres by the comparison of the calculated EXAFS signal and that isolated from the full EXAFS spectrum using the method of Fourier filtration of MFT. This nonlinear fitting was performed using the IFFEFIT-1.2.11 program package [25]. The phases and scattering amplitudes of the photoelectron wave necessary for the construction of the model spectrum were calculated using the FEFF7 program [26] and atomic coordinates of the compounds with similar atomic structures. The goodness-of-fit function (Q), which was minimized by determining the parameters of the nearest environment structure, was calculated using the equation

$$Q(\%) = \frac{\sum\left[k\chi_{exp}(k) - k\chi_{th}(k)\right]^2}{\sum\left[k\chi_{exp}(k)\right]^2} \times 100.$$

The C, H, and N elemental analyses were conducted on a Carlo Erba Instruments TCM 480 instrument. The metals were analyzed using gravimetry. Melting points were measured on a Koffler hot-stage. The IR spectra of the samples were recorded on a Varian 3100-FTIR Excalibur instrument in a range of 4000–400 cm^{-1} using the attenuated total reflection (ATR) method. The specific magnetic susceptibility was determined by the relative Faraday method at room temperature using $Hg[Co(CNS)_4]$ as a standard for calibration.

The XRD data for the single crystals of complexes **Ia**, **Ib**, and **Ic** grown in a chloroform–methanol (2 : 1) mixture were obtained using the synchrotron radiation source of the Kurchatov Institute Russian Research Center at the Protein station [27] at 100 K in direct geometry ($\theta = 0°$). Totally, about 500 frames were recorded in the ϕ scan mode. An absorption correction was applied using the Scala program [28]. The XRD data were integrated using the iMOSFLM program [29]. The structures were solved and refined using the SHELXTL program [30]. The structures were refined and analyzed by full-matrix least squares for F^2 in the Olex2 program [31] using the SHELXL program package. The hydrogen atoms were localized according to the geometry and residual electron density peaks. The experimental characteristics and crystallographic data for complexes **Ia**–**Ic** are presented in Table 1.

The coordinates of atoms and temperature factors for complexes **Ia**, **Ib**, and **Ic** were deposited with the Cambridge Crystallographic Data Centre (CIF files CCDC nos. 1910746, 1910747, and 1910748, respectively; deposit@ccdc.cam.ac.uk or http://www.ccdc.cam.ac.uk/data_request/cif).

RESULTS AND DISCUSSION

The Cu(II), Ni(II), and Co(II) complexes, **Ia**–**Ic** and **IIa**–**IIc**, were synthesized by the CM and EM methods as a continuation of the study [4] of the complexation ability of the tetradentate azomethine compounds, the derivatives of 2-(*N*-tosylamino)benzaldehyde and the corresponding dioxadiamines H_2L^1 and H_2L^2.

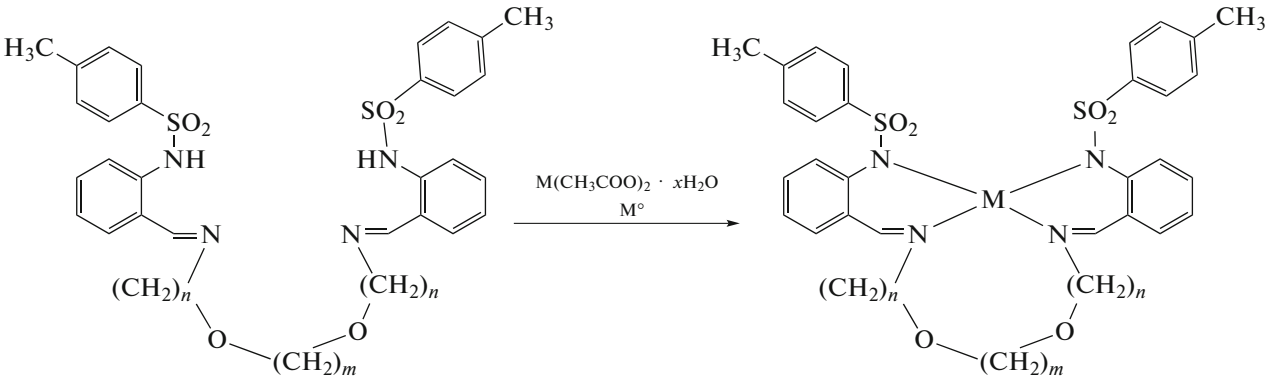

$m = 2$, $n = 2$ H_2L^1
$m = 4$, $n = 3$ H_2L^2

$m = 2$, $n = 2$ (**I**)
$m = 4$, $n = 3$ (**II**)
M = Cu (a), Ni (b), Co (c)

Table 1. Crystallographic parameters and experimental data for the crystals of complexes **Ia** · X, **Ib** · X, and **Ic** · X (X = MeOH)

Parameters	Value		
	Ia · MeOH	**Ib** · MeOH	**Ic** · MeOH
Empirical formula	$C_{35}H_{40}N_4O_7S_2Cu$	$C_{35}H_{40}N_4O_7S_2Ni$	$C_{35}H_{40}N_4O_7S_2Co$
FW	756.37	751.54	751.76
Color, habitus	Lilac-red plates	Light green plates	Red-brown plates
Sample size, mm	0.2 × 0.1 × 0.1	0.2 × 0.1 × 0.1	0.3 × 0.2 × 0.1
Temperature, K	100		
Crystal system	Triclinic		
Space group	$P\bar{1}$		
a, Å	11.096(2)	11.285(2)	11.303(2)
b, Å	12.542(3)	12.374(3)	12.493(3)
c, Å	12.896(3)	12.925(3)	12.891(3)
α, deg	80.35(3)	79.96(3)	80.13(3)
β, deg	76.37(3)	76.22(3)	75.61(3)
γ, deg	81.890(3)	81.84(3)	81.92(3)
V, Å^3	1709.7(7)	1716.5(7)	1728.0(7)
Z	2	2	2
ρ_{calc}, g/cm^3	1.469	1.454	1.568
μ, cm^{-1}	1.10	1.00	1.08
F(000)	790	788	850
Synchrotron radiation (λ, Å)	Rayonix SX165 CCD (0.7937)		
θ, deg	1.8/ 31.0	1.8/31.0	1.8/31.0
Range of indices *h, k, l*	$-14 \le h \le 14$, $-16 \le k \le 16$, $-16 \le l \le 16$	$-14 \le h \le 14$, $-15 \le k \le 16$, $-16 \le l \le 16$	$-14 \le h \le 14$, $-16 \le k \le 16$, $-16 \le l \le 16$
Total number of measured reflections	39067	27855	46043
Number of independent reflections	7783	7768	7810
Number of reflections with $I > 2\sigma(I)$	7326	7250	7211
R_{int}	0.029	0.072	0.034
$(\sin\theta/\lambda)_{max}$, Å^{-1}	0.648	0.594	0.648
Number of refined parameters	446	446	447
R ($I > 2\sigma(I)$)	$R_1 = 0.038$ $wR_2 = 0.138$	$R_1 = 0.044$ $wR_2 = 0.144$	$R_1 = 0.034$ $wR_2 = 0.098$
$\Delta\rho_{max}/\Delta\rho_{min}$, *e*/Å^3	0.72/–0.81	0.58/–0.73	0.50/–0.43

The structures of tetradentate ligands H_2L^1 and H_2L^2 and complexes **Ia**–**Ic** and **IIa**–**IIc** were determined by elemental analysis, IR spectroscopy, ^{1}H NMR spectroscopy (for compound **I**), EXAFS spectroscopy, and XRD. According to the elemental analysis data, complexes **Ia**–**Ic** have the compositions $ML^1 \cdot MeOH$ and complexes **IIa**–**IIc** are of the ML^2 composition regardless of the synthesis method. Their IR spectral characteristics are the same. However, "milder" conditions for the synthesis of the complexes and an increase in their yields by 5–10% are advantages of the EM method over the CM method [32–35]. The ν(NH) absorption bands of ligands H_2L^1 and H_2L^2 in a range of 2700–3150 cm^{-1} disappear from the IR spectra of the complexes. The ν(CH=N) absorption bands at 1638 (H_2L^1) and 1634 cm^{-1} (H_2L^2) decrease insignificantly to 1618–1629 cm^{-1} upon the formation of complexes **Ia**–**Ic** and **IIa**–**IIc**. The

absorption bands of ligand H_2L^1 at 1336 ($\nu_{as}(SO_2)$) and 1156 cm^{-1} ($\nu_s(SO_2)$) and of ligand H_2L^2 at 1338 ($\nu_{as}(SO_2)$) and 1154 cm^{-1} ($\nu_s(SO_2)$) in the spectra of complexes **Ia**–**Ic** decrease to 1256–1288 ($\nu_{as}(SO_2)$) and 1133–1135 cm^{-1} ($\nu_s(SO_2)$), and those for complexes **IIa**–**IIc** decrease to 1254–1288 ($\nu_{as}(SO_2)$) and 1127–1136 cm^{-1} ($\nu_s(SO_2)$), respectively. This spectral behavior indicates in favor of the deprotonation of ligands H_2L^1 and H_2L^2 and formation of chelate structures **Ia**–**Ic** and **IIa**–**IIc**.

The structures of compounds **Ia**–**Ic** · X (X = MeOH) were determined by XRD. The crystals of compounds **Ia** · X, **Ib** · X, and **Ic** · X are isostructural. Compounds ML^1 · MeOH (**Ia** · X, **Ib** · X, and **Ic** · X) are similar and resemble the earlier described complexes ZnL · MeOH and CdL · $CHCl_3$ [4]. Insignificant distinctions in the structures of the compounds are caused, most likely, by a change in the atomic radius of the complexing metal atom. The molecular structure of complex **Ia** is shown in Fig. 1. The bond lengths and bond angles in the coordination polyhedra of the metals are presented in Table 2.

In the molecules of ML^1, the macrocyclic ligand coordinates the metal atom via the tetradentate chelate mode by four nitrogen atoms to form the polyhedron as a distorted tetrahedron. The polyhedron of Cu(II) is somewhat more flattened (the dihedral angle between the planar fragments N(1)M(1)N(3) and N(2)M(1)N(4) is 69.1° in **Ia**, 79.2° in **Ib**, and 76.9° in **Ic**).

The M–N bond lengths in complexes **Ia**–**Ic** are fairly close, and some regular elongation of the M(1)–N(3) and M(1)–N(4) bonds is observed in the series Cu–Ni–Co (Table 2).

Two six-membered metallocycles and one eleven-membered metallocycle are formed upon the coordination of the organic ligand to the metal ion. The

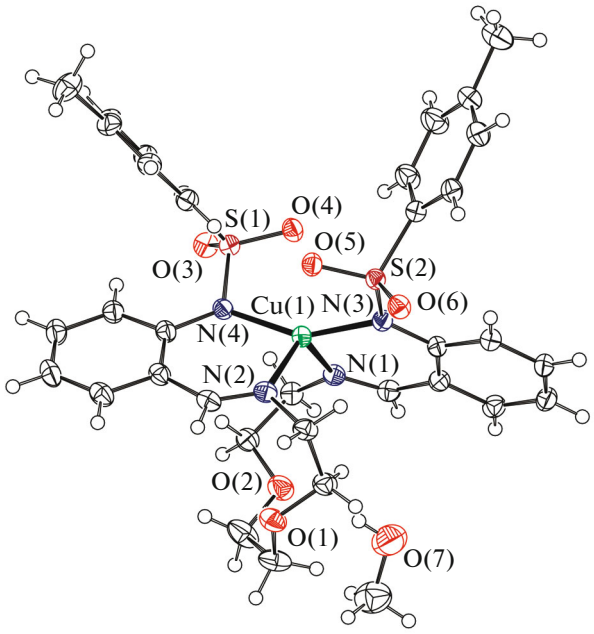

Fig. 1. Molecular structure of complex **Ia** in the atomic representation by atomic shift ellipsoids of 50% probability.

structures of the six-membered chelate cycles are close to planar due to the conjugation with the corresponding phenyl ring.

The eleven-membered metallocycles containing the dioxadiamine fragment are characterized by the nonplanar conformation and contain no multiple bonds.

The view of the eleven-membered cycle in complex **Ia** is presented in Fig. 2. The presence of the metal atom leads to a significant deformation of the cycles. The metallocycles are pseudo-centrosymmetric if the

Table 2. Bond lengths and bond angles in the coordination polyhedra of complexes **Ia**–**Ic**

Bond	*d*, Å		
	Ia (M = Cu)	**Ib** (M = Ni)	**Ic** (M = Co)
M(1)–N(1)	2.0160(16)	2.0131(16)	2.0193(15)
M(1)–N(2)	2.0447(16)	2.0137(16)	2.0264(15)
M(1)–N(3)	1.9504(15)	1.9781(15)	2.0007(14)
M(1)–N(4)	1.9465(16)	1.9760(16)	1.9939(15)
Angle	ω, deg		
N(1)M(1)N(2)	117.32(6)	105.91(6)	112.35(6)
N(3)M(1)N(1)	92.19(6)	91.41(7)	92.18(6)
N(3)M(1)N(2)	103.44(6)	105.76(7)	107.86(6)
N(4)M(1)N(1)	101.65(7)	102.53(7)	105.91(6)
N(4)M(1)N(2)	92.46(7)	91.58(7)	93.03(6)
N(4)M(1)N(3)	151.28(6)	153.96(6)	144.83(6)

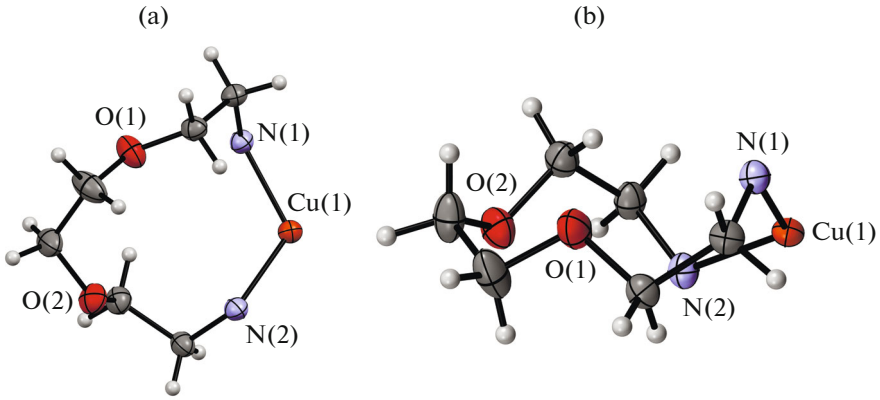

Fig. 2. View of the eleven-membered metallochelate cycle in the molecule of complex **Ia** along the crystallographic axes (a) *c* and (b) *b*.

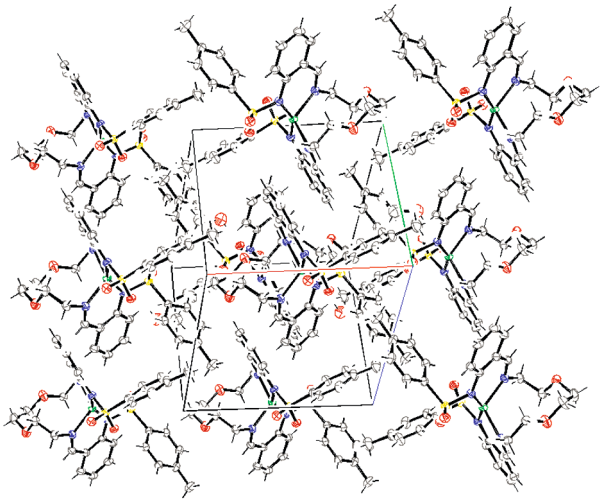

Fig. 3. Molecular packing in the crystal lattice of complex **Ia**.

CH_2–CH_2 fragment connecting the oxygen atoms is opposite to the metal atom. The torsion angles involving the metal atom are in the *gauchi–gauchi–gauchi* conformation, and other angles have the *gauchi–trans–gauchi* and *gauchi–gauchi–trans* conformations.

Planar layers are formed from the complex molecules in all structures (Fig. 3). Solvate methanol molecules are arranged between the layers and form with the complex molecules strong intermolecular hydrogen bonds with similar parameters (Table 3). No specific interactions between the complex molecules were observed in the single crystals of the compounds.

The local atomic structures of complexes **IIa**–**IIc** were determined from analysis of the corresponding XANES (X-ray absorption near edge structure) and EXAFS *K*-edge absorption spectra. The X-ray Cu-, Ni-, and Co*K*-edge absorption spectra and their first derivatives for complexes **IIa**, **IIb**, and **IIc** are shown in Fig. 4. All XANES spectra exhibit the pronounced pre-edge structure A (insets in Fig. 4) caused by the 3*d*–4*p* mixing of the atomic orbitals of the metal, whose intensity is directly proportional to the degree of filling of the vacant 3*d* shell and symmetry of the environment. The shapes of the XANES spectra and especially the first edge derivatives consisting of two broadened maxima are typical of the complexes with the tetrahedral environment of the absorbing atom.

The quantitative characteristics of the local atomic structures of complexes **IIa**, **IIb**, and **IIc** were obtained from an analysis of the EXAFS Cu-, Ni-, and Co*K*-edge absorption spectra of these compounds. Figure 5 shows that all MFT EXAFS consist of the major peak about $r = 1.56$ Å, which unambiguously corresponds to the scattering on the nearest coordination spheres consisting of the nitrogen atoms of the ligands and the peaks at longer distances corresponding to the scattering on the subsequent coordination spheres.

Table 3. Parameters of hydrogen bonds in the crystal structures of compounds **Ia**–**Ic**

Compound	D–H···A	Distance, Å			Angle DHA, deg
		D–H	H···A	D···A	
Ia	O(7)–H(7*A*)···O(1)	0.82	1.97	2.780(3)	170
Ib	O(7)–H(7*A*)···O(1)	0.82	1.97	2.772(3)	167
Ic	O(7)–H(7*A*)···O(1)	0.82	1.98	2.790(2)	171

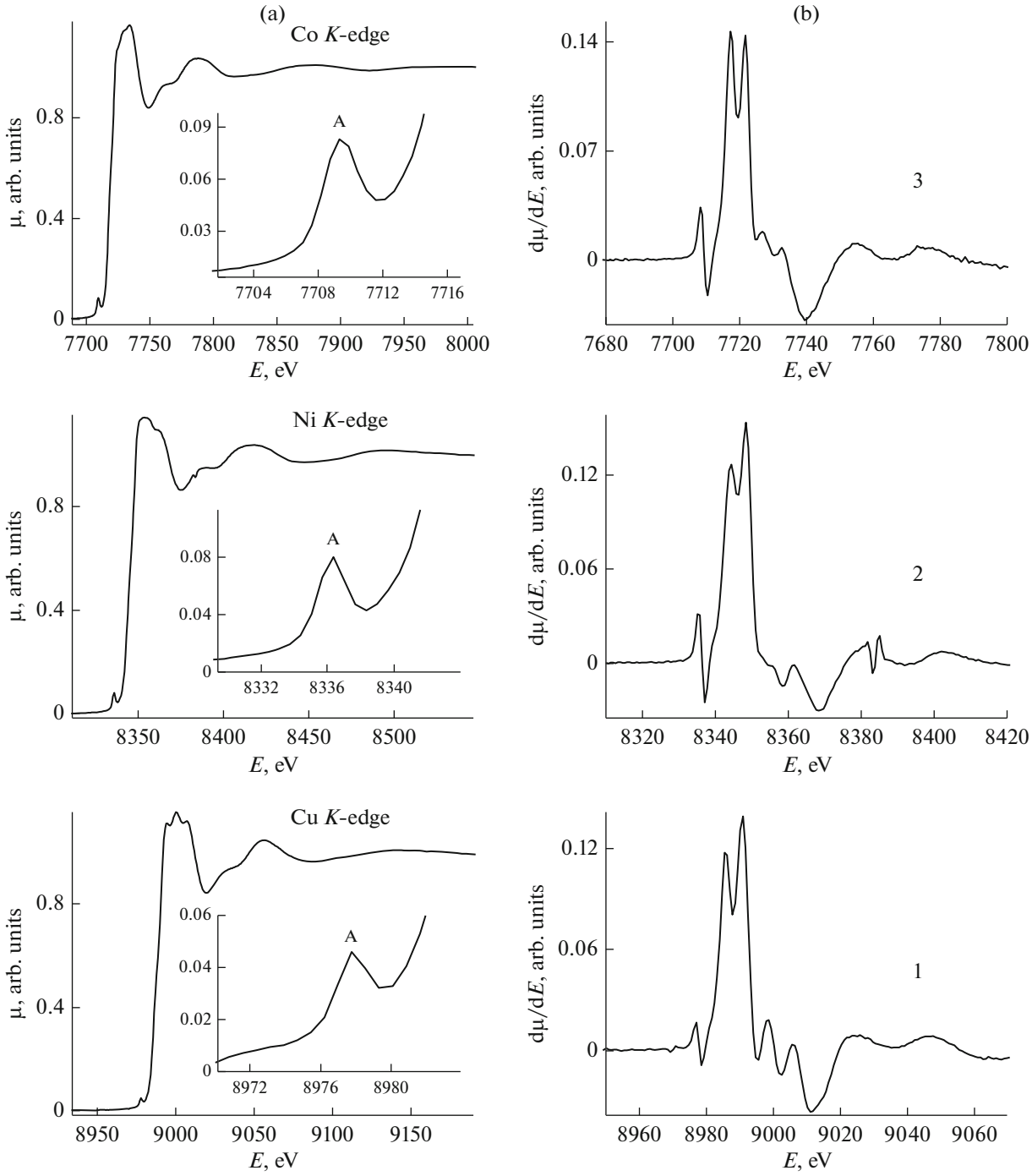

Fig. 4. (a) X-ray Cu-, Ni-, and Co*K*-edge absorption spectra, where the pre-edge range A is shown in insets, and (b) the first derivatives of the edges dμ/d*E* for complexes (1) **IIa**, (2) **IIb**, and (3) **IIc**.

The results of the calculations of the parameters of the local atomic environment of the metal ions in complexes **IIa**–**IIc** with the chosen corresponding models of the atomic structure of the coordination node (Table 4) indicate similar structural parameters of the coordination site in these complexes. Four nitrogen atoms are arranged around the metal ions at an average distance of 1.98 Å **(IIa)**, 2.00 Å **(IIb)**, and 2.01 Å **(IIc)**. These distances correspond to the bond lengths for compounds **IIa**, **IIb**, and **IIc** determined from the XRD data. The Debye–Waller factors for the nearest coordination spheres are somewhat higher than the typical values for these distances, but this increase can be explained by averaging of the bond lengths of the nearest coordination sphere for one-sphere fitting. Thus, the local atomic structures of the

Table 4. Structural data for the local atomic structures of complexes **IIa**, **IIb**, and **IIc** obtained by the one-sphere fitting of the EXAFS data*

Compound	*N*	*R*, Å	σ^2, Å^2	Atom	*Q*, %
IIa	4	1.98	0.0045	N	0.4
IIb	4	2.00	0.0040	N	1.4
IIc	4	2.01	0.0045	N	4.0

*R are interatomic distances, N is the coordination number, σ^2 is the Debye–Waller factor, and Q is the goodness-of-fit function (the approximation range is shown in the footnote).

coordination sites in complexes **Ia**–**Ic** and **IIa**–**IIc** are characterized by similar values of the structural parameters indicating that the structures are independent of the value of *m*.

The complexes of the **I**–**II** type are paramagnetic. The values of μ_{eff} are 1.94–2.0 (Cu), 3.19–3.30 (Ni), and 4.70–4.72 μ_B (Co) at room temperature and remain nearly unchanged with the temperature decrease, indicating the mononuclear tetrahedral structures of the complexes.

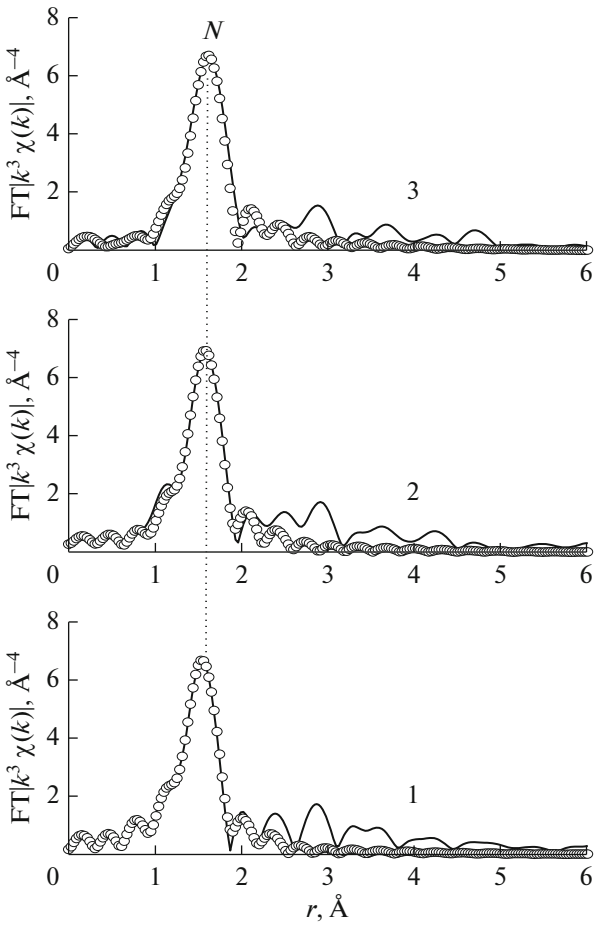

Fig. 5. MFT for (1) Cu-, (2) Ni-, and (3) Co*K*-edge absorption spectra for complexes **IIa**, **IIb**, and **IIc** (solid line is experiment, and theoretical values are shown by empty circles).

To conclude, the Cu(II), Ni(II), and Co(II) complexes of the tetradentate azomethine compounds, the condensation products of 2-(*N*-tosylamino)benzaldehyde with 3,4-dioxa-1,8-octanediamine and 4,9-dioxa-1,12-dodecanediamine, were synthesized by the chemical and electrochemical methods. It follows from the data of X-ray absorption spectroscopy that four nitrogen atoms are arranged around the metal ions at average distances of 1.98–2.01 Å in the complexes with 4,9-dioxa-1,12-dodecanediamine. The X-ray structural studies for the metal complexes with 3,4-dioxa-1,8-octanediamine show that the complexes of the $ML^1 \cdot MeOH$ composition and their crystals are isostructural with insignificant distinctions in distances and angles in the coordination polyhedra. In the molecules of the complexes, the macrocyclic ligands coordinate the metal atom by four nitrogen atom via the tetradentate chelate mode to form the polyhedron as a distorted tetrahedron.

ACKNOWLEDGMENTS

The equipment of the unique scientific setup "Kurchatov Synchrotron Radiation Source" supported by the Ministry of Education and Science of the Russian Federation (project no. RFMEFI61914X0002) was used. The IR and ^{1}H NMR spectra were recorded using the equipment of the Center for Collective Use "Molecular Spectroscopy."

FUNDING

This work was supported by the Southern Federal University.

CONFLICT OF INTEREST

The authors declare that they have no conflicts of interest.

REFERENCES

1. Cozzi, P.G., *Chem. Soc. Rev.*, 2004, vol. 33, p. 410. https://doi.org/10.1039/b307853c
2. Gupta, K.C. and Sutar, A.K., *Coord. Chem. Rev.*, 2008, vol. 252, nos 12–14, p. 1420. https://doi.org/10.1016/j.ccr.2007.09.005
3. Pawanoji, A.A. and Mehta, B.H., Imper. *J. Interdiscipl. Res.*, 2016, vol. 2, no. 12, p. 448.

4. Burlov, A.S., Vlasenko, V.G., Garnovskii, D.A., et al., *Russ. J. Inorg. Chem.*, 2014, vol. 59, p. 721. https://doi.org/10.1134/S0036023614070031
5. Burlov, A.S., Vlasenko, V.G., Koshchienko, Yu.V., et al., *Polyhedron*, 2018, vol. 144, p. 249. https://doi.org/10.1016/j.poly.2018.01.020
6. Burlov, A.S., Mal'tsev, E.I., Vlasenko, V.G., et al., *Polyhedron*, 2017, vol. 133, p. 231. https://doi.org/10.1016/j.poly.2017.05.045
7. Lysakova, T.P., Burlov, A.S., Vlasenko, V.G., et al., *Russ. J. Coord. Chem.*, 2016, vol. 42, p. 701. https://doi.org/10.1134/S1070328416110075
8. Burlov, A.S., Vlasenko, V.G., Koshchienko, Y.V., et al., *Russ. J. Coord. Chem.*, 2016, vol. 42, p. 267. https://doi.org/10.1134/S1070328416030027
9. Burlov, A.S., Ikorskii, V.N., Nikolaevskii, S.A., et al., *Russ. J. Inorg. Chem.*, 2008, vol. 53, no. 10, p. 1566. https://doi.org/10.1134/S0036023608100082
10. Burlov, A.S., Vlasenko, V.G., Koshchienko, Yu.V., et al., *Polyhedron*, 2018, vol. 154, p. 123. https://doi.org/10.1016/j.poly.2018.07.053
11. Burlov, A.S., Koshchienko, Yu.V., Ikorskii, V.N., et al., *Russ. J. Inorg. Chem.*, 2006, vol. 51, no. 7, p. 1065. https://doi.org/10.1134/S0036023606070096
12. Burlov, A.S., Uraev, A.I., Ikorskii, V.N., et al., *Russ. J. Gen. Chem.*, 2008, vol. 78, no. 6, p. 1230. https://doi.org/10.1134/S1070363208060224
13. Barton, J.K., *Science*, 1986, vol. 233, p. 727.
14. Burrows, C.J. and Muller, J.G., *Chem. Rev.*, 1998, vol. 98, p. 1109. https://doi.org/10.1021/cr960421s
15. Erkkila, K.E., Odom, D.T., and Barton, J.K., *Chem. Rev.*, 1999, vol. 99, p. 2777. https://doi.org/10.1021/cr9804341
16. Santini, C., Pellei, M., Gandin, V., et al., *Chem. Rev.*, 2014, vol. 114, no. 1, p. 815. https://doi.org/10.1021/cr400135x
17. Peng Li, Mei Ju Niu, Min Hong, et al., *J. Inorg. Biochem.*, 2014, vol. 137, p. 101. https://doi.org/10.1016/j.jinorgbio.2014.04.005
18. Singh, K., Barwa, M.S., and Tyagi, P., *Eur. J. Med. Chem.*, 2006, vol. 41, p. 147. https://doi.org/10.1016/j.ejmech.2005.06.006
19. Fonkui, T.Y., Ikhile, M.I., Ndinteh, D.T., et al., *Trop. J. Pharm. Res.*, 2018, vol. 17, p. 2507. https://doi.org/10.4314/tjpr.v17i12.29
20. Abd El Halim, H.F., Mohamed, G.G., and Anwar, M.N., *Appl. Organomet. Chem.*, 2018, vol. 32. https://doi.org//10.1002/aoc.3899
21. Chernova, N.I., Ryabokobylko, Yu.S., Brudz', V.G., and Bolotin, B.M., *Zh. Org. Khim.*, 1971, vol. 7, no. 8, p. 1680.
22. Tuck, D.G., *Pure Appl. Chem.*, 1979, vol. 51, no. 10, p. 2005. https://doi.org/10.1351/pac197951102005
23. Chernyshov, A.A., Veligzhanin, A.A., and Zubavichus, Ya.V., *Nucl. Instr. Meth. Phys. Res. A*, 2009, vol. 603, p. 95. https://doi.org/10.1016/j.nima.2008.12.167
24. Kochubei, D.I., Babanov, Yu.A., Zamaraev, K.I., et al., *Rentgenospektral'nyi metod izucheniya struktury amorfnykh tel: EXAFS-spektroskopiya* (X-ray Spectral Method for Investigation of Structures of Amorphous Solids: EXAFS Spectroscopy), Novosibirsk: Nauka SO, 1988.
25. Newville, M., *J. Synchrotron Rad.*, 2001, vol. 8, p. 96. https://doi.org/10.1107/S0909049500016290
26. Zabinski, S.I., Rehr, J.J., Ankudinov, A., and Alber, R.C., *Phys. Rev. B*, 1995, vol. 52, p. 2995. https://doi.org/10.1103/PhysRevB.52.2995
27. Lazarenko, V.A., Dorovatovskii, P.V., Zubavichus, Y.V., et al., *Crystals*, 2017, vol. 7, no. 11, p. 325. https://doi.org/10.3390/cryst7110325
28. Evans, P.R., *Acta Crystallogr., Sect. D: Struct. Biol.*, 2006, vol. 62, p. 72. https://doi.org/10.1107/S0907444905036693
29. Battye, T.G., Kontogiannis, L., Johnson, O., et al., *Acta Crystallogr., Sect. D: Struct. Biol.*, 2011, vol. 67, p. 271. https://doi.org/10.1107/S0907444910048675
30. Sheldrick, G.M., *Acta Crystallogr., Sect. A: Found. Crystallogr.*, 2008, vol. 64, no. 1, p. 112. https://doi.org/10.1107/S0108767307043930
31. Dolomanov, O.V., Bourhis, L.J., Gildea, R.J., et al., https://doi.org/10.1107/S0021889808042726
32. Kharisov, B.I., Blanco, L.M., Garnovskii, A.D., et al., *Polyhedron*, 1998, vol. 17, nos. 2–3, p. 381. https://doi.org/10.1016/S0277-5387(97)00284-2
33. Kharisov, B.I., Garnovskii, D.A., Blanco, L.M., Burlov, A.S., et al., *Polyhedron*, 1999, vol. 18, no. 7, p. 985. https://doi.org/10.1016/S0277-5387(98)00383-0
34. Vlasenko, V.G., Garnovskii, D.A., Aleksandrov, G.G., et al., *Polyhedron*, 2019, vol. 157, p. 6. https://doi.org/10.1016/j.poly.2018.09.065
35. Garnovskii, D.A., Vlasenko, V.G., Aleksandrov, G.G., et al., *Russ. J. Coord. Chem.*, 2018, vol. 44, p. 596. https://doi.org/10.1134/S1070328418100032

Translated by E. Yablonskaya